

## Isotope effect in niobium self-diffusion

W. Bussmann and Chr. Herzig

*Institut für Metallforschung der Universität Münster, Münster, W. Germany*

H. A. Hoff and J. N. Mundy

*Materials Science Division, Argonne National Laboratory, 9700 South Cass Avenue, Argonne, Illinois 60439*

(Received 8 January 1981)

Measurements of the isotope effect in niobium self-diffusion have been made over the temperature range 1900 °C to near the melting point (2468 °C). The measurements were made by simultaneous diffusion of  $^{95}\text{Nb}$  and  $^{92}\text{Nb}$  isotopes from a thin surface layer and subsequent sectioning. The ratio of  $^{92}\text{Nb}$  to  $^{95}\text{Nb}$  in each section was determined using a well-type Ge(Li) detector of high efficiency. The low values of the measured isotope effect are similar to other bcc metals (Na,  $\alpha$ - and  $\delta$ -Fe, Cr, and  $\beta$ -Zr); however, the temperature dependence is different.

### I. INTRODUCTION

Measurements of the isotope effect  $E$  for self-diffusion in metals have proved valuable in establishing mechanisms of diffusion.<sup>1-3</sup> The experimentally measured quantity  $E$  is defined by

$$E = \frac{D_\alpha/D_\beta - 1}{(m_\beta/m_\alpha)^{1/2} - 1} = f\Delta K, \quad (1)$$

where  $D_\alpha$  and  $D_\beta$  are the diffusion coefficients of the two isotopes  $\alpha$  and  $\beta$  with masses  $m_\alpha$  and  $m_\beta$ ;  $f$  is the correlation factor which for self-diffusion is a numerical constant depending only on the diffusion mechanism and the crystal structure;  $\Delta K$  is the fraction of the kinetic energy at the saddle point associated with motion in the jump direction that belongs to the diffusing atom. In cases where more than one mechanism contributes simultaneously to diffusion,  $E$  may be written as

$$E = \sum p_i f_i \Delta K_i, \quad (2)$$

where  $p_i$  is the proportion of diffusion occurring by means of mechanism  $i$ .

The measured values of  $E$  can clearly be a complex function of several parameters and not simple to interpret.<sup>4</sup> This problem was helped in the case of isotope-effect measurements on metals with a face-centered-cubic structure by other experiments on the same elements. High-temperature equilibrium measurements<sup>5</sup> had established that the dominant defects were single vacancies, and an analysis of self-diffusion measurements made over a wide temperature range<sup>1,6</sup> showed that, in general, at all temperatures up to the melting temperature one diffusion process dominates. This information together with the measured values of  $E$  established that the principal mechanism of diffusion in fcc metals was atomic hopping by means of single vacancies. The analy-

ses<sup>1,2,4</sup> also established that for fcc metals  $0.95 \leq \Delta K_{1v} < 1$ , and that at temperatures close to the melting temperature a second process, probably divacancies, also contributed to diffusion.

In metals with a body-centered-cubic structure,  $E$  has been measured in sodium,<sup>7</sup>  $\alpha$ -Fe (Refs. 8-11) and  $\delta$ -Fe (Refs. 8 and 9), chromium,<sup>12</sup> and  $\beta$ -zirconium.<sup>13</sup> The interpretation of the data has proved troublesome,<sup>1,3,8-21</sup> not only because of both the low values of  $E$  and their temperature dependence, but also because, in general, the knowledge of the type and concentration of lattice defects established for fcc metals has been lacking for bcc metals. An analysis of self-diffusion coefficients in bcc metals<sup>6,22</sup> measured over a wide temperature range shows that, with the exception of chromium, the isotope measurements have been performed in a temperature region where more than only a simple vacancy diffusion process is expected to occur. Interpreting the results in connection with the divacancy mechanism, further complications arise. Migration of a divacancy in a bcc lattice may involve three different divacancy configurations and two different saddle points.<sup>17,19,20</sup> The high values of  $p_{1v}$  and  $\Delta K_{1v}$  found in fcc metals allowed an unambiguous interpretation of the measured values of  $E$ . For bcc metals the strong dependence of  $p_i$  on temperature and values of  $E$ , which require  $\Delta K_i \leq 0.6$ , has made interpretation of isotope-effect measurements very difficult.

The concept of expecting the detailed understanding of physical properties obtained on a number of elements to apply to all other elements belonging to that group is common to many fields, and has also been applied to the field of diffusion and defects in metals.<sup>1,4,5,23</sup> The similarity of diffusion parameters<sup>1</sup> in different fcc metals would appear to justify this procedure for metals with this structure. However, for metals with a bcc structure the diffusion parameters span a wide range of

values<sup>22</sup> and it is less clear that prototypes can be found. There is one subset of bcc metals, those in group V and group VI, which do have diffusion parameters with close similarity to those found for fcc metals (cf. Tables II and III of Ref. 6). The high-temperature bcc phases of group-IV metals show, however, a different diffusion behavior than other bcc metals.<sup>13,23</sup>

In the group-V and -VI metals isotope-effect measurements have been made only on chromium.<sup>12</sup> The values of  $E$  were low and showed a strong temperature dependence ( $E=0.3$  at  $T_m/T=1.02$  and  $E=0.5$  at  $T_m/T=1.24$ , where  $T_m$  is the melting temperature). The diffusion coefficients were measured over a temperature range  $T_m/T=1.02$  to 1.57 and no deviation from a straight Arrhenius line was apparent. This would suggest that the values of  $E$  refer to one mechanism. The low and temperature-dependent values of  $E$  would require a temperature dependence of  $f_i$  and  $\Delta K_i$ . The one mechanism for which  $f_i$  could vary between 0.35 and 0.5 is the divacancy mechanism, when one takes into account the different divacancy configurations.<sup>2,20</sup> The value  $f_{2v}=0.35$  is for the 1N-2N-1N-type jump process, while the values  $f_{2v}=0.5$  is for the 2N-4N-2N process.<sup>20</sup> (1N, 2N, and 4N refer to the first, second, and fourth nearest-neighbor configurations of the divacancy.) The experimental results<sup>12</sup> appear to require that in the relatively narrow range of temperature measurement, the divacancy mechanism changes from one type to the other. The extension of the measurements to lower temperatures was not possible with the existing experimental techniques. The present work on niobium has been made in order to examine the isotope effect for self-diffusion in another bcc transition metal in a wide temperature range to get more information on possible diffusion mechanisms. Earlier attempts to make these measurements using a half-life method to discriminate between the simultaneously diffused isotopes, <sup>95</sup>Nb and <sup>90</sup>Nb, were unsuccessful because of low concentrations of the radioactive impurities <sup>89</sup>Zr and <sup>95</sup>Zr.<sup>24</sup> The present study applies an energy discrimination technique using a well-type Ge(Li) with high efficiency.<sup>13</sup>

## II. EXPERIMENTAL METHODS

The basic method was to observe the simultaneous diffusion of the radioisotopes <sup>95</sup>Nb and <sup>92</sup>Nb from a thin surface layer into the bulk of a niobium single crystal. The solution of the diffusion equation for the experimental conditions is, for the isotope <sup>95</sup>Nb,

$$C_{95}(x) = [S_{95}/(\pi D_{95} t)^{1/2}] \exp(-x^2/4D_{95} t), \quad (3)$$

where  $C_{95}(x)$  is the specific activity of the <sup>95</sup>Nb tracer at a distance  $x$  from the surface,  $t$  is the time of the diffusion anneal,  $S_{95}$  is the tracer concentration of isotope <sup>95</sup>Nb per unit area at  $x=0$  and  $t=0$ , and  $D_{95}$  is the diffusion coefficient of isotope <sup>95</sup>Nb. A similar expression can be written for the isotope <sup>92</sup>Nb and the ratio of the specific activities ( $C_{92}/C_{95}$ ) can be shown to be

$$\ln\left(\frac{C_{92}}{C_{95}}\right) = \text{const} - \ln C_{95} \left(1 - \frac{D_{92}}{D_{95}}\right). \quad (4)$$

Plots of  $\ln(C_{92}/C_{95})$  vs  $\ln(C_{95})$  were used to obtain the slope  $1 - D_{92}/D_{95}$  and from Eq. (1) values of  $E$  were derived.

The techniques used in the sample and isotope preparation and the diffusion annealing were largely the same as described in Ref. 22, while serial sectioning of the samples and the evaluation of the isotope effect were different. The single-crystal samples (9.5 mm diameter, 3 mm long) were cut from single-crystal niobium rods supplied by the Materials Research Corporation. The <sup>95</sup>Nb ( $T_{1/2} = 35d$ ) was purchased from Oak Ridge National Laboratory in the form of niobium oxalate in oxalic acid. The maximum level of <sup>95</sup>Zr impurity content present in the niobium isotope used in the present work was 1.5%. The <sup>92</sup>Nb ( $T_{1/2} = 10.2d$ ) was made in the Argonne cyclotron by the <sup>89</sup>Y( $\alpha, n$ )<sup>92</sup>Nb reaction. The <sup>92</sup>Nb was separated from the yttrium by the Argonne Analytical Chemistry Group using ion exchange techniques. The major impurity in the yttrium was tantalum and this was also removed in order to obtain a thin layer of radioactive salt on the surface of the sample. The <sup>92</sup>Nb was extracted as a chloride and converted to oxalate before mixing with the <sup>95</sup>Nb. The proportions were adjusted so that the radioactive counts were approximately the same for both isotopes at the time the sections from the diffusion anneal were counted.

All diffusion anneals were made in an ultrahigh vacuum electron beam furnace at pressures  $\leq 2 \times 10^{-6}$  Pa. Samples from the high, intermediate, and low anneal temperatures were analyzed for oxygen ( $\sim 60$  at. ppm) and carbon ( $\sim 500$  at. ppm). The samples used in the earlier work contained much lower content of interstitial impurity because of the decarburization and deoxygenation procedures that were used. However, the earlier work showed no dependence of diffusion on interstitial content so the samples were made from *as*-supplied niobium.

Two samples were annealed together and the anneal temperature measured by observing with an optical pyrometer the "black-body hole" defined by the two active niobium sample surfaces and the inside of a tantalum ring which holds the

samples 1 mm apart. A sketch of the sample configuration (for four samples) is shown in Ref. 22. The annealing of two as opposed to four samples required new temperature calibrations. The anneal temperature in the previous work was that of the measured central black space defined by the two active surfaces. The diffusion coefficient for this anneal temperature was the geometric mean of the  $D$  values obtained from each sample. In the present work calibration samples were made with black-body holes spark-machined 1 mm below and parallel to the active surface. Following the diffusion anneal the calibration samples were arranged in the same geometry and with the temperature of the central space adjusted to that of the anneal temperature to which the individual sample temperatures were then compared.

Following the diffusion anneal the samples were sent to the University of Münster for sectioning and isotope counting. The samples were reduced in diameter and sectioned on a microtome into 3–10  $\mu\text{m}$  thick slices, depending on the depth of the diffusion profile, to get about 20 sections for each sample. The sections were weighed on a microbalance and dissolved in equal volumes of a  $\text{HNO}_3$  (47%),  $\text{HF}$  (3%), and  $\text{H}_2\text{O}$  (50%) solution. The first sections in the diffusion profile were diluted to  $8 \times 10^4$  counts/min in order to avoid pile-up effects and large dead-time corrections in the counting equipment. The diluted volumes were brought back to the same volume as for the other sections by addition of the above solution containing the appropriate mass of inactive niobium.

The  $\gamma$  radiation from the  $^{92}\text{Nb}$  and  $^{95}\text{Nb}$  was discriminated and counted using a well-type  $\text{Ge}(\text{Li})$  detector in combination with a 4K multichannel analyzer (MCA) and a PDP 8 computer.<sup>13</sup> The absolute efficiency of the detector was  $\sim 7.3\%$  for the 765-keV peak of  $^{95}\text{Nb}$ . The  $\gamma$  spectrum from one of the latter sections of a diffusion profile is

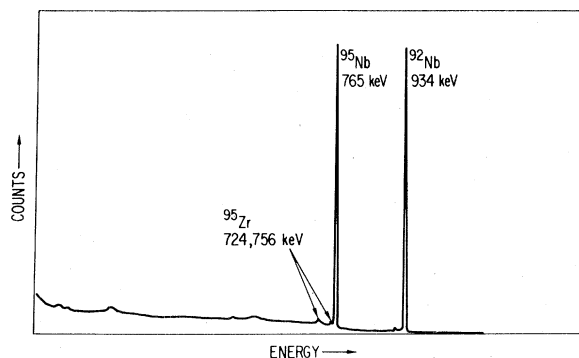


FIG. 1.  $\gamma$  spectra taken from a section  $\sim 3\sqrt{Dt}$  from the initial surface of a diffusion sample.

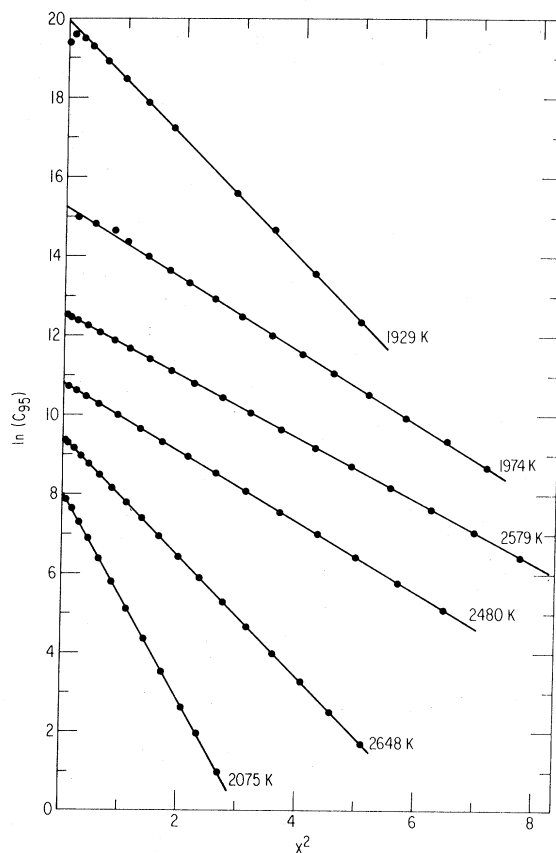


FIG. 2. Concentration profiles as a function of penetration. The individual profiles have been scaled for clarity. The abscissa scale is in units of  $10^{-4} \text{ cm}^2$  for the 2579 and 2648-K profiles,  $10^{-5} \text{ cm}^2$  for the 2075 and 2480-K profiles, and  $5 \times 10^{-6} \text{ cm}^2$  for the 1929 and 1974-K profiles.

shown in Fig. 1. In earlier sections the  $^{95}\text{Zr}$  peak was not observed. The energy resolution of the counting system was 3.2 keV full width at half maximum (FWHM) for the 1.332-MeV peak of  $^{60}\text{Co}$  and sufficient to separate the 756-keV peak of  $^{95}\text{Zr}$  from the 765-keV peak of  $^{95}\text{Nb}$ . The spectra of the individual sections were stored on tape. The positions of the  $\gamma$  peaks in the MCA were reproducible to  $\pm 0.2$  keV over a period of weeks. The individual count rates of  $^{92}\text{Nb}$  and  $^{95}\text{Nb}$  were determined by setting an energy window 906–955 keV and 761–773 keV. Corrections for half-life and for Compton background were performed using pure  $^{92}\text{Nb}$  and  $^{95}\text{Nb}$  standards. With the exception of the last two or three sections of a diffusion profile, where only  $5 \times 10^5$  counts were collected, the statistical counting error was less than 0.1%.

### III. EXPERIMENTAL RESULTS

Examples of the penetration profiles obtained for the  $^{95}\text{Nb}$  isotope are shown in Fig. 2. The data

TABLE I. Diffusion of  $^{95}\text{Nb}$  and  $^{92}\text{Nb}$  in niobium.

Temperature (K)	Anneal time (s)	$D$ ( $\text{cm}^2 \text{s}^{-1}$ )	$E$
$2672.9 \pm 7.8$	$1.068 \times 10^3$	$(1.516 \pm 0.002) \times 10^{-8}$	$0.346 \pm 0.010$
$2656.0 \pm 8.3$	$3.243 \times 10^3$	$(1.659 \pm 0.014) \times 10^{-8}$	$0.398 \pm 0.011$
$2647.8 \pm 16.7$	$1.068 \times 10^3$	$(1.593 \pm 0.002) \times 10^{-8}$	$0.417 \pm 0.014$
$2605.0 \pm 10.0$	$3.243 \times 10^3$	$(1.405 \pm 0.005) \times 10^{-8}$	$0.400 \pm 0.011$
$2579.0 \pm 7.5$	$4.005 \times 10^3$	$(8.035 \pm 0.015) \times 10^{-9}$	$0.374 \pm 0.012$
$2554.7 \pm 10.5$	$4.005 \times 10^3$	$(5.895 \pm 0.009) \times 10^{-9}$	$0.398 \pm 0.020$
$2479.7 \pm 7.2$	$1.188 \times 10^3$	$(2.380 \pm 0.001) \times 10^{-9}$	$0.369 \pm 0.020$
$2341.2 \pm 9.2$	$1.468 \times 10^4$	$(8.864 \pm 0.007) \times 10^{-10}$	$0.435 \pm 0.027$
$2319.2 \pm 13.6$	$1.468 \times 10^4$	$(6.946 \pm 0.008) \times 10^{-10}$	$0.455 \pm 0.014$
$2211.6 \pm 6.2$	$2.733 \times 10^4$	$(2.099 \pm 0.006) \times 10^{-10}$	$0.458 \pm 0.023$
$2086.3 \pm 6.2$	$2.927 \times 10^4$	$(4.332 \pm 0.048) \times 10^{-11}$	$0.433 \pm 0.023$
$2074.6 \pm 8.1$	$2.927 \times 10^4$	$(3.283 \pm 0.015) \times 10^{-11}$	$0.485 \pm 0.012$
$1974.0 \pm 5.7$	$8.702 \times 10^4$	$(1.547 \pm 0.014) \times 10^{-11}$	$0.431 \pm 0.023$
$1929.0 \pm 13.9$	$8.702 \times 10^4$	$(9.757 \pm 0.095) \times 10^{-12}$	$0.430 \pm 0.026$

from the concentration profiles were least-squares fitted to obtain the values of the diffusion coefficients given in Table I and shown in Fig. 3. The error in  $D$  is the anneal time error added to the error in the slope of the  $\ln C_{95}$  vs  $x^2$  plots. The

errors in the temperature measurements were determined as part of the calibration procedure. The line shown in Fig. 3 illustrates a new fit of the data of Ref. 22 using a Statistical Analysis System (SAS) routine.<sup>25</sup> The new fit improves the chi-square value by a factor of 2 and gives

$$D = 1.5 \times 10^{-2} \exp \left[ - \left( \frac{3.67 \pm 0.27 \text{ eV}}{kT} \right) \right] + 4.6 \exp \left[ - \left( \frac{4.59 \pm 0.34 \text{ eV}}{kT} \right) \right]. \quad (5)$$

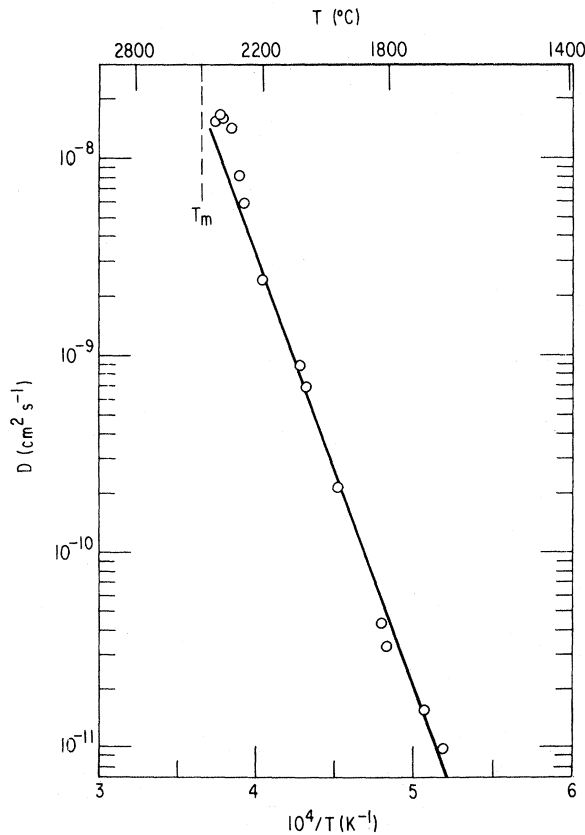


FIG. 3. Niobium self-diffusion coefficient plotted as a function of  $1/T$  ( $\text{K}^{-1}$ ). The solid line is from the data of Ref. 22.

The present data agree well except at the highest temperatures where they are systematically high. The discrepancy is within the error of the previous measurements ( $\pm 20^\circ$ ) and so a recalibration of the earlier work which used a different geometry has not been attempted.

Examples of the experimental plots of  $\ln(C_{92}/C_{95})$  vs  $\ln(C_{95})$  are shown in Fig. 4. Null-effect experiments showed zero slopes within the error of the measurements. The values of  $E$  obtained from the slopes of the  $\ln(C_{92}/C_{95})$  vs  $\ln(C_{95})$  plots are given in Table I and plotted in Fig. 5 as a function of the homologous temperature  $T_m/T$ . The isotope effect shows a distinct temperature dependence qualitatively comparable to that in sodium. The values of  $E$  for niobium appear to decrease below  $T_m/T \sim 1.3$ ; however, further data at lower temperatures would be needed to confirm this trend. Since the earliest measurements of  $E$  in sodium<sup>7</sup> suggested that  $E$  vs  $T_m/T$  could be well fitted by a parabola, this fit was also probed for the present data, and is shown by the line in Fig. 5. It should be emphasized, however, that this is an empirical fit only, with no physical justification at present for this functional form.

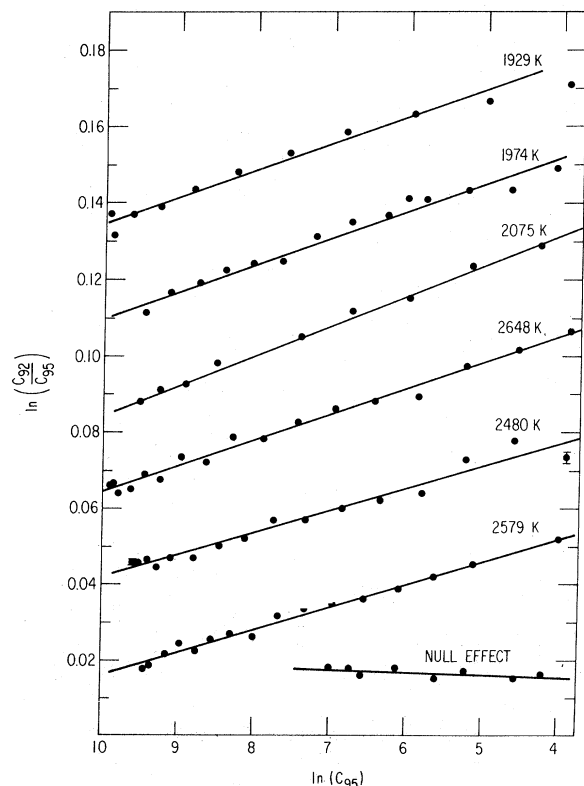


FIG. 4. Diffusion of  $^{95}\text{Nb}$  and  $^{92}\text{Nb}$  in niobium.

#### IV. DISCUSSION

As already noted, the interpretation of the results of isotope effect experiments in bcc metals has proved difficult. The values of  $E$  are obviously temperature dependent, and at high temperatures they are lower than expected for vacancy-type mechanisms. The present data on niobium

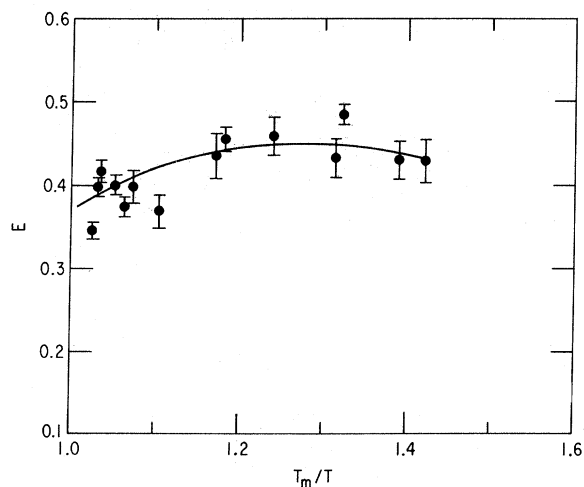


FIG. 5. Isotope effect in niobium self-diffusion as a function of  $T_m/T$ .

follow this pattern and unambiguous interpretation will again prove impossible. The data will be discussed in terms of Eq. (2). Earlier discussions<sup>7,12,13</sup> also made use of Eq. (2), so both the validity and value of the equation will first be examined.

For the most commonly discussed mechanism, single vacancies together with divacancies (single-divacancy), Eq. (2) has been usually written<sup>1-3,13,21,26</sup>

$$E = (f\Delta K)_{\text{eff}} = f_{1v} \Delta K_{1v} \frac{D_{1v}^T}{D^T} + g_{2v} \Delta K_{2v} \frac{D_{2v}^T}{D^T}, \quad (6)$$

where the superscript  $T$  refers to the tracer diffusion coefficient and where, in general,  $g_{2v} > f_{2v}$  and is dependent both on the assumed divacancy configurations and the various possible migration paths. The same equation has been written<sup>27</sup> for the case  $\Delta K_{1v} = \Delta K_{2v} = 1$ . The effective correlation factor can also be written<sup>2,28</sup> as

$$f_{\text{eff}} = f_{1v} \frac{D_{1v}^{\text{SD}}}{D^{\text{SD}}} + f_{2v} \frac{D_{2v}^{\text{SD}}}{D^{\text{SD}}}, \quad (7)$$

where the superscript SD refers to the random-walk self-diffusion coefficient (i.e.,  $D^T = fD^{\text{SD}}$ ). Equation (7) can be rewritten in terms of  $D^T$  and gives

$$f_{\text{eff}} = \frac{f_{1v}f_{2v}}{f_{1v}D_{2v}^T/D^T + f_{2v}D_{1v}^T/D^T}. \quad (8)$$

In Fig. 6(a) a fit to the measured data of  $E$  of sodium<sup>7</sup> is compared to  $f_{\text{eff}}$  from both Eqs. (6) and (8). The values of  $f_{1v} = 0.727$  and  $f_{2v} = 0.50$  were used and the values of  $D_{iv}^T/D^T$  taken from Ref. 7. Values of  $E_{\text{eff}}$  calculated<sup>2</sup> using Eq. (6) (values of  $D_{1v}$ ,  $D_{2v}$ ,  $f_{1v}$ , and  $f_{2v}$  were obtained from Göltz *et al.*<sup>29</sup>) are also shown in Fig. 6(a). The differences between Eqs. (6) and (8) are small. The figure shows the dominant effect of changing values of  $\Delta K$ ; however, a good fit to the data is not achieved by Eq. (6), mainly because the sign of the curvature is opposite to that of the experimental results.

In Fig. 6(b) the present niobium work is compared to the curve for  $f_{\text{eff}}$  determined from Eq. (6) [ $f_{1v} = 0.727$ ,  $f_{2v} = 0.50$ , and  $D_{iv}^T/D^T$  ratios obtained from Eq. (5)]. A suitable adjustment of values of  $\Delta K_{iv}$  allows values of  $E_{\text{eff}}$  to be calculated that bisect the niobium data in a similar way to that shown for sodium in Fig. 6(a). However, there are problems with such a procedure beyond simply the poor quality of the fit that is obtained. If the single-divacancy mechanism is used to interpret the data then  $f_{1v} > g_{2v}$  and  $\Delta K_{1v} \geq K_{2v}$ , so that we expect  $E_{\text{eff}}$  to decrease with increasing temperature if  $\Delta K_{iv}$  are temperature independent.<sup>2</sup> If at the low end of the temperature range the single-vacancy process were dominant,  $E_{\text{eff}}$  would be

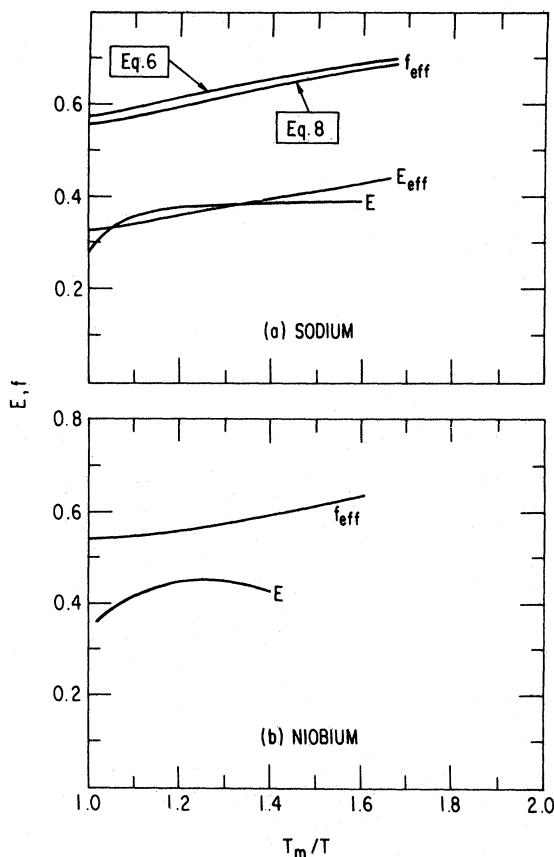


FIG. 6. Comparison of computed values of the correlation factor for sodium (a) and niobium (b).

come independent of temperature. At  $T_m/T = 1.3$  we find from Eq. (5) that only one-third of the diffusion occurs by the low-temperature process. This means that  $E_{eff}$  should still increase in the range  $T_m/T > 1.3$ . The measured values of  $E$ , however, do not show this behavior. From this concept it would appear difficult to fit the niobium isotope-effect data with a single-divacancy interpretation using the hitherto accepted values of  $f_i$ ,  $\Delta K_{iv}$ , and  $p_i$ .

There has been recent evidence from both a comparison of NMR and tracer-diffusion measurements<sup>30</sup> and from a comparison of quasielastic neutron scattering and tracer-diffusion measurements<sup>29</sup> that in sodium a single-divacancy mechanism is the appropriate interpretation. The line shown for  $E_{eff}$  in Fig. 6(a) (sodium) was de-

termined from the fit to the sodium-tracer data obtained by Göltz *et al.*<sup>29</sup> The fit takes account of jumps by single vacancies and divacancies jumping by both  $1N-2N-1N$  and  $2N-4N-2N$  processes. As already noted, a good fit to the sodium data for  $E$  is not obtained. The comparison of the tracer diffusion and NMR measurements was made over the temperature range 195–273 K. At 273 K the fit to the NMR data<sup>30</sup> gives  $D_{1v}^{SD}/D^{SD} \sim 0.14$ , which is in strong contrast to the value  $D_{1v}^{SD}/D^{SD} \sim 0.43$  obtained from the fit of Göltz *et al.*<sup>29</sup> to the tracer-diffusion data. If the curvature in the Arrhenius line found for the sodium data by both methods has the same physical origin and is to be interpreted solely by single-divacancy processes, one would expect a better agreement in the value of  $D_{1v}^{SD}/D^{SD}$  obtained by the different techniques.

The difficulty remains how to interpret the temperature dependence of the measurements of  $E$  in niobium and sodium. In the context of the single-divacancy model, an explanation can only come from a distinct temperature dependence of  $\Delta K_{iv}$ , a problem which has not yet been treated theoretically in bcc metals.

## V. CONCLUSIONS

The isotope effect in niobium is strongly temperature dependent at temperatures near the melting point. This dependence seems not to be interpretable in terms of a single-divacancy type process. The agreement between the measured and the calculated curve of the isotope effect remains poor even if one takes into account a temperature dependence of the type of the divacancy jump process. Further interpretation will require careful measurements of defect properties over a wide range of temperatures and a better theoretical understanding of  $\Delta K_{iv}$  in bcc metals.

## ACKNOWLEDGMENTS

We are grateful for the radiochemical separations made by E. Huff of the Analytical Chemistry Group, Argonne National Laboratory, and for the  $\alpha$  irradiation made by M. Oselka, Chemistry Division, Argonne National Laboratory. We thank R. W. Siegel for helpful discussions. This work was supported by the U. S. Department of Energy and the Deutsche Forschungsgemeinschaft.

<sup>1</sup>N. L. Peterson, *J. Nucl. Mater.* **69-70**, 3 (1978).

<sup>2</sup>H. Mehrer, *J. Nucl. Mater.* **69-70**, 38 (1978).

<sup>3</sup>Chr. Herzig, H. Ecksele, W. Bussmann, and D. Cardis, *J. Nucl. Mater.* **69-70**, 61 (1978).

<sup>4</sup>A. Seeger and H. Mehrer, in *Vacancies and Interstitials in Metals*, edited by A. Seeger, D. Schumacher, W. Schilling, and J. Diehl (North-Holland, Amsterdam, 1970) p. 1.

- <sup>5</sup>R. W. Siegel, *J. Nucl. Mater.* **69-70**, 117 (1978).
- <sup>6</sup>J. N. Mundy, S. J. Rothman, N. Q. Lam, H. A. Hoff, and L. J. Nowicki, *Phys. Rev. B* **18**, 6566 (1978).
- <sup>7</sup>J. N. Mundy, *Phys. Rev. B* **3**, 2431 (1971).
- <sup>8</sup>C. M. Walter and N. L. Peterson, *Phys. Rev.* **178**, 922 (1969).
- <sup>9</sup>D. Graham, *J. Appl. Phys.* **40**, 2386 (1969).
- <sup>10</sup>C. O. DeGonzales and N. E. W. de Reça, *J. Phys. Chem. Solids*, **32**, 1067 (1971).
- <sup>11</sup>V. Irmer and M. Feller-Kniepmeier, *J. Appl. Phys.* **43**, 953 (1972).
- <sup>12</sup>J. N. Mundy, C. W. Tse, and W. D. McFall, *Phys. Rev. B* **13**, 2349 (1976).
- <sup>13</sup>Chr. Herzig and H. Eckeler, *Z. Metallkd.* **70**, 215 (1979).
- <sup>14</sup>R. C. Brown, J. Worster, N. H. March, R. C. Perrin, and R. Bullough, *Philos. Mag.* **23**, 555 (1971).
- <sup>15</sup>R. V. Hesketh, *Philos. Mag.* **24**, 1233 (1971).
- <sup>16</sup>M. Feit, *Philos. Mag.* **25**, 769 (1972).
- <sup>17</sup>P. S. Ho, *Philos. Mag.* **26**, 1429 (1972).
- <sup>18</sup>M. Feit, *Phys. Rev. B* **5**, 2145 (1972).
- <sup>19</sup>P. S. Ho, *Phys. Rev. B* **7**, 3550 (1973).
- <sup>20</sup>H. Mehrer, *J. Phys. F* **3**, 543 (1973).
- <sup>21</sup>N. L. Peterson, *Comments Solid State Phys.* **8**, 93 (1978).
- <sup>22</sup>R. E. Einziger, J. N. Mundy, and H. A. Hoff, *Phys. Rev. B* **17**, 440 (1978).
- <sup>23</sup>N. L. Peterson, *Comments Solid State Phys.* **8**, 107 (1978).
- <sup>24</sup>R. E. Einziger and J. N. Mundy, *Phys. Rev. B* **17**, 449 (1978).
- <sup>25</sup>A. J. Barr, J. H. Goodnight, J. P. Sall, J. T. Helwig, and P. S. Keinhardt, *SAS User's Guide*, SAS Institute, Inc., Raleigh, North Carolina 27605 (1979).
- <sup>26</sup>N. L. Peterson, in *Diffusion in Solids—Recent Developments*, edited by A. S. Nowick and J. J. Burton, (Academic, New York, 1975), p. 116.
- <sup>27</sup>H. Bakker, *Phys. Status Solidi B* **44**, 369 (1971).
- <sup>28</sup>D. Wolf, *J. Appl. Phys.* **49**, 2752 (1978).
- <sup>29</sup>G. Göltz, A. Heidemann, H. Mehrer, A. Seeger, and D. Wolf, *Philos. Mag. A* **41**, 723 (1980).
- <sup>30</sup>G. Brünner, O. Kanert, and D. Wolf, *Solid State Commun.* **33**, 569 (1980).